

The viscoelastic Kolmogorov flow: eddy viscosity and linear stability

By G. BOFFETTA¹, A. CELANI², A. MAZZINO³,
A. PULIAFITO² AND M. VERGASSOLA⁴

¹Dipartimento di Fisica Generale, Università di Torino and Istituto Nazionale di Fisica Nucleare, Sez. di Torino, V. Giuria 1, 10125 Torino, Italy

²CNRS, INLN, 1361 Route des Lucioles, 06560 Valbonne, France

³INFM – Dipartimento di Fisica, Università di Genova, and Istituto Nazionale di Fisica Nucleare, Sez. di Genova, Via Dodecaneso 33, 16146 Genova, Italy

⁴CNRS URA 2171, Inst. Pasteur, 28 rue du Dr. Roux, 75724 Paris Cedex 15, France.

(Received 25 May 2004 and in revised form 6 October 2004)

The stability properties of the laminar Kolmogorov flow of a viscoelastic Oldroyd-B fluid are investigated both analytically and numerically. Linear stability with respect to large-scale perturbations is studied by means of multiple-scale analysis. This technique yields an effective diffusion equation for the large-scale perturbation where the effective (eddy) viscosity can be computed analytically. Stability amounts to the positive definiteness of the eddy-viscosity tensor as a function of the Reynolds and the Deborah numbers. Two main results emerge from our analysis: (i) at small fluid elasticity, the flow is more stable than in the Newtonian case; (ii) at high elasticity, the flow is prone to elastic instabilities, occurring even at vanishing Reynolds number. The hypothesis of scale separation is verified up to moderate elasticity, as checked by numerical integration of the exact linearized equations by the Arnoldi method. Finally, it is shown that the addition of a stress diffusivity counteracts the effect of elasticity, in agreement with simple physical arguments.

1. Introduction

Flow instabilities are a classical subject in fluid dynamics (Drazin & Reid 1981) and the theoretical study of their occurrence in polymer solutions and melts is of paramount importance for several industrial applications (see e.g. Petrie & Denn 1976; Larson 1992; Shaqfeh 1996). A satisfactory understanding of these flow transitions entails taking account of the viscoelastic behaviour of such fluids.

A spectacular consequence of viscoelasticity is the drag reduction effect: addition of minute amounts (a few tenths of p.p.m. in weight) of long-chain soluble polymers to water leads to a strong reduction (up to 80%) of the power necessary to maintain a given throughput in a channel (Toms 1949; Lumley 1969; Virk 1975). Despite the vast number of studies on the subject, the understanding of drag reduction by polymers is still incomplete (Lumley 1969; Virk 1975; Nadolink & Haigh 1995; Sureshkumar, Beris & Handler 1997; Sreenivasan & White 2000).

Recently, some theoretical works have been aimed at establishing a link between drag reduction and the stability properties of the flow (Govindarajan, L'vov & Procaccia 2001; Stone, Waleffe & Graham 2002). Our goal here is to give further evidence that the seed of drag reduction is found at the very initial stage of the

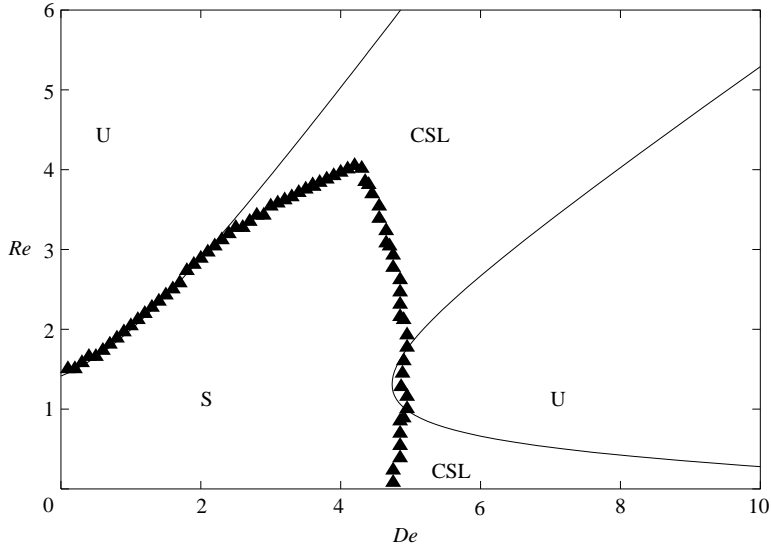


FIGURE 1. The stability portrait as predicted by multiple-scale analysis (solid line) and computed by numerical solution of the exact linearized equations (triangles). In the region denoted by U the flow is unstable, in that denoted by S it is stable. Inside the area denoted by CSL the flow is stable with respect to large-scale perturbations, but unstable with respect to generic perturbations.

successive instabilities which lead to a fully developed turbulent regime. In this framework, the possible occurrence of drag reduction can be detected by investigating how the stability of the flow changes upon polymer injection.

The basic flow we focus on is the extension to viscoelastic fluids of the well-known Kolmogorov flow (Arnold & Meshalkin 1960). Boffetta, Celani & Mazzino (2004) have shown that the fully developed turbulent regime of this flow displays drag reduction. Similarly to the Newtonian case (Meshalkin & Sinai 1961), the evolution of large-scale perturbations – the most unstable ones for moderate fluid elasticity – can be formally described by an effective viscous dynamics. Instabilities are thus associated with the loss of positive definiteness of the eddy-viscosity tensor, whose analytical expression can be explicitly derived from the equations of motion by means of multiple-scale analysis (Bensoussan, Lions & Papanicolaou 1978). In the Newtonian case, the eddy-viscosity tensor is a function of the Reynolds number, Re , and long-wave transverse instabilities occur above the threshold $Re_c = \sqrt{2}$ (Meshalkin & Sinai 1961). In the viscoelastic case studied here, the effective viscosity depends on both the Reynolds and the Deborah, De , numbers. (The latter is related to the typical polymer relaxation time.) The boundary between stable and unstable regions in the Re – De phase space is determined by the parameter values such that the viscosity tensor loses its positive definiteness.

We anticipate our main result in figure 1, showing the phase-space portrait obtained by multiple-scale methods (see §4). For moderate De , the critical Reynolds number is an increasing function of the Deborah number: this demonstrates the stabilization of the flow field induced by the polymers (Govindarajan *et al.* 2001; Stone *et al.* 2002). The asymptotic result obtained for large-scale perturbations is confirmed by the numerical solution of the full linear stability problem (see §6). Discrepancies in figure 1 between perturbative and numerical results are due to lack of scale separation,

i.e. instabilities occurring at small or moderate scales, which cannot be captured by multiple-scale methods.

2. The Oldroyd-B model

The Oldroyd-B model is based on the assumption that a polymer solution can be treated as a dilute suspension of elastic dumbbells, i.e. pairs of microscopic beads connected by harmonic springs (Bird *et al.* 1987). The elastic constant of the spring is inversely proportional to the typical polymer relaxation time τ , controlling the response of the polymers to the stretching effects exerted by the local shear in the flow.

The distance between the two beads, here denoted by \mathbf{R} , evolves according to the stochastic equation

$$\dot{\mathbf{R}} = (\mathbf{R} \cdot \partial)\mathbf{u} - \frac{1}{2\tau}\mathbf{R} + \sqrt{\frac{R_0^2}{\tau}}\boldsymbol{\xi}. \quad (2.1)$$

On the right-hand side, the first term is the stretching/compression term, originating from the spatial variation of the flow experienced at \mathbf{R} . The second is a relaxation contribution, where one considers only the largest – and thus the most effective in the interaction with the flow – characteristic time τ . The last term, $\boldsymbol{\xi}$, is a white-in-time random process mimicking the effect of thermal noise on the polymers. R_0 denotes the equilibrium spring length, in the absence of advecting flow. This description remains valid and no other physical effects (such as the nonlinearity of the springs) need to be taken into account as long as we consider moderate polymer elongations.

Averaging (2.1) over the statistics of the thermal noise $\boldsymbol{\xi}$, the following evolution equation for the conformation tensor $\boldsymbol{\sigma} \equiv \langle \mathbf{R}\mathbf{R} \rangle / R_0^2$ is obtained:

$$\partial_t \boldsymbol{\sigma} + (\mathbf{u} \cdot \partial)\boldsymbol{\sigma} = (\partial\mathbf{u})^T \cdot \boldsymbol{\sigma} + \boldsymbol{\sigma} \cdot (\partial\mathbf{u}) - \frac{1}{\tau}(\boldsymbol{\sigma} - \mathbb{1}), \quad (2.2)$$

where $(\partial\mathbf{u})_{\alpha\beta} \equiv \partial_\alpha u_\beta$ and $\text{tr}\partial\mathbf{u} = \partial \cdot \mathbf{u} = 0$.

The dynamical effect of the polymers on the flow is due to the elastic contribution to the stress tensor. In the Oldroyd-B model (see e.g. Bird *et al.* 1987), that is for Hookean springs, this contribution per unit density is

$$\boldsymbol{\tau} = \frac{\nu(1-\beta)}{\tau}(\boldsymbol{\sigma} - \mathbb{1}), \quad (2.3)$$

where ν is the total kinematic viscosity of the solution, $\nu\beta$ and $\nu(1-\beta)$ are the contribution of the solvent and of the polymers to the total viscosity, respectively. Here we have introduced the dimensionless parameter $\beta = \eta_s / (n_p k_B \Theta \tau + \eta_s)$, n_p being the polymer concentration, k_B denoting the Boltzmann constant, Θ the temperature and η_s the dynamic viscosity of the solvent. The resulting momentum equations are

$$\partial_t \mathbf{u} + (\mathbf{u} \cdot \partial)\mathbf{u} = -\partial p + \nu\beta \partial^2 \mathbf{u} + \frac{\nu(1-\beta)}{\tau} \partial \cdot (\boldsymbol{\sigma} - \mathbb{1}) + \mathbf{f}. \quad (2.4)$$

3. Basic equilibrium state

As a first step in investigating the effect of polymers on the stability of the flow, we need to find a basic equilibrium state that will then be perturbed and the resulting perturbation growth evaluated exploiting a multiple-scale analysis.

Finding a basic equilibrium state for a generic forcing \mathbf{f} is already a formidable problem for the Navier–Stokes equations without polymers. The task is further complicated here by the additional term in (2.4) and the coupling with (2.2).

The problem simplifies for $\mathbf{f} \equiv (f(z), 0, 0)$ that induces a parallel flow $\mathbf{U} = (U(z), 0, 0)$, trivially annihilating the nonlinear term in (2.4). A further substantial simplification is introduced by the viscoelastic version of Squire's theorem (Squire 1933), which states that for parallel flows the most unstable perturbations are two-dimensional. We shall therefore restrict consideration to the two-dimensional flow (u_x, u_z) , without prejudicing generality. We further specialize by assuming $f(z) = F_0 \cos(z/L)$, producing the well-known Kolmogorov flow (Arnold & Meshalkin 1960) $U(z) \equiv u_x(z) = V \cos(z/L)$, $u_z = 0$.

The conformation tensor at equilibrium has then the form

$$\boldsymbol{\sigma} = \begin{pmatrix} 1 + 2\tau^2(\partial_z U)^2 & \tau \partial_z U \\ \tau \partial_z U & 1 \end{pmatrix} = \begin{pmatrix} 1 + 2\tau^2 \frac{V^2}{L^2} \sin^2\left(\frac{z}{L}\right) & -\tau \sin\left(\frac{z}{L}\right) \\ -\tau \frac{V}{L} \sin\left(\frac{z}{L}\right) & 1 \end{pmatrix}, \quad (3.1)$$

and $F_0 = \nu V/L^2$.

4. Multiple-scale analysis

Let us now consider the linearized equations for the system of perturbations $(\mathbf{w}, q, \boldsymbol{\zeta})$ of the basic state $(\mathbf{u}, p, \boldsymbol{\sigma})$. Equations (2.2) and (2.4), together with the incompressibility condition, lead to

$$\partial \cdot \mathbf{w} = 0, \quad (4.1)$$

$$\partial_t \mathbf{w} + \partial \cdot (\mathbf{u}\mathbf{w} + \mathbf{w}\mathbf{u}) = -\partial q + \nu\beta \partial^2 \mathbf{w} + \nu(1 - \beta)\tau^{-1} \partial \cdot \boldsymbol{\zeta}, \quad (4.2)$$

$$\partial_t \boldsymbol{\zeta} + \partial \cdot (\mathbf{u}\boldsymbol{\zeta} + \boldsymbol{\zeta}\mathbf{u}) = (\partial \mathbf{u})^T \cdot \boldsymbol{\zeta} + (\partial \mathbf{w})^T \cdot \boldsymbol{\sigma} + \boldsymbol{\zeta} \cdot (\partial \mathbf{u}) + \boldsymbol{\sigma} \cdot (\partial \mathbf{w}) - \tau^{-1} \boldsymbol{\zeta}. \quad (4.3)$$

We shall study the behaviour of perturbations with a characteristic length scale much larger than L , the periodicity of the basic flow. The ratio of small to large scales will be denoted by ϵ . In the spirit of multiple-scale expansions (Bensoussan *et al.* 1978), we introduce a set of *slow variables* ($\tilde{\mathbf{x}} = \epsilon \mathbf{x}, \tilde{t} = \epsilon^2 t$) in addition to the *fast variables* (\mathbf{x}, t) of evolution of the basic flow. The scaling of the slow time \tilde{t} is suggested by physical reasons: we are expecting a diffusive behaviour at large scales and the relation between space and time is thus assumed to be quadratic.

The multiple-scale technique (Bensoussan *et al.* 1978) treats slow and fast variables as independent, in order to capture the secular effects shaping the macroscopic dynamics. The differential operators appearing in (4.1)–(4.3) transform according to the chain rule as

$$\partial_i \rightarrow \partial_i + \epsilon \tilde{\partial}_i, \quad \partial_t \rightarrow \partial_t + \epsilon^2 \tilde{\partial}_t, \quad (4.4)$$

where $i = 1, 2$ denotes x and z . In the following, we assume that the amplitude of the fields in (4.1)–(4.3) are small enough to neglect nonlinear effects (their analysis will be reported elsewhere). The amplitudes can then be rescaled out so that the fields \mathbf{w} , q and $\boldsymbol{\zeta}$ are expanded as

$$\left. \begin{aligned} \mathbf{w} &= \mathbf{w}^{(0)}(z, t, \tilde{x}, \tilde{z}, \tilde{t}) + \epsilon \mathbf{w}^{(1)}(z, t, \tilde{x}, \tilde{z}, \tilde{t}) + \epsilon^2 \mathbf{w}^{(2)}(z, t, \tilde{x}, \tilde{z}, \tilde{t}) + \dots, \\ q &= q^{(0)}(z, t, \tilde{x}, \tilde{z}, \tilde{t}) + \epsilon q^{(1)}(z, t, \tilde{x}, \tilde{z}, \tilde{t}) + \epsilon^2 q^{(2)}(z, t, \tilde{x}, \tilde{z}, \tilde{t}) + \dots, \\ \boldsymbol{\zeta} &= \boldsymbol{\zeta}^{(0)}(z, t, \tilde{x}, \tilde{z}, \tilde{t}) + \epsilon \boldsymbol{\zeta}^{(1)}(z, t, \tilde{x}, \tilde{z}, \tilde{t}) + \epsilon^2 \boldsymbol{\zeta}^{(2)}(z, t, \tilde{x}, \tilde{z}, \tilde{t}) + \dots, \end{aligned} \right\} \quad (4.5)$$

where all the functions have the same periodicity as the basic state.

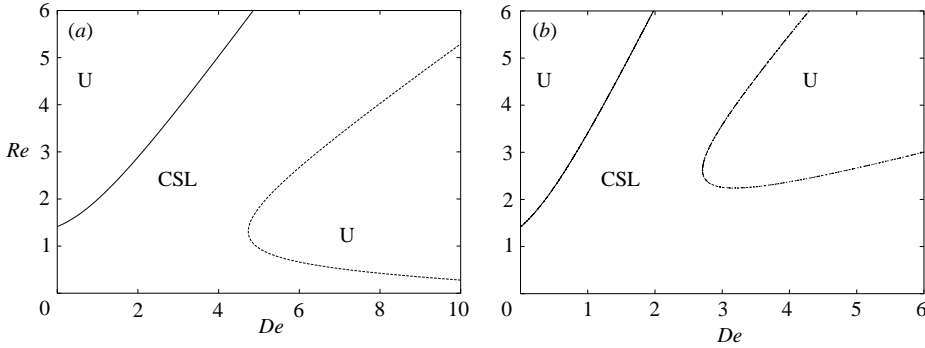


FIGURE 2. The stability diagram obtained by multiple-scale analysis for (a) $\beta=0.77$ and (b) $\beta=0.167$, with the notation of figure 1. Higher β corresponds to very low polymer concentrations while lower β means high concentrations.

Inserting (4.5) into (4.1)–(4.3) and exploiting (4.4), we end up with equations in which both fast and slow variables appear. By a further average over z , we obtain a set of equations involving large-scale fields only, i.e. depending on \tilde{x} and \tilde{t} .

Using incompressibility, the large-scale velocity perturbations $\langle \mathbf{w}^{(0)} \rangle$ can be described via the large-scale stream function $\Psi(\tilde{x}, \tilde{z}, \tilde{t})$ as

$$\langle w_x^{(0)} \rangle = \tilde{\partial}_z \Psi, \quad \langle w_z^{(0)} \rangle = -\tilde{\partial}_x \Psi. \tag{4.6}$$

The evolution equation for Ψ is obtained as a solvability condition (Fredholm alternative) at order ϵ^2 . After lengthy, but straightforward, algebra we obtain

$$\tilde{\partial}_t \tilde{\Delta} \Psi = \nu_{\alpha\beta} \tilde{\partial}_\alpha^2 \tilde{\partial}_\beta^2 \Psi, \tag{4.7}$$

where $\mathbf{v} = \nu \mathbb{1} + \mathbf{v}^e$, and

$$\begin{aligned} \nu_{xx}^e &= \frac{V^2 \{-L^2 + \nu(1-\beta)\tau[3 + (1+2\beta)(\nu\tau/L^2)]\}}{2\nu}, & \nu_{zz}^e &= 0, \\ \nu_{xz}^e &= \nu_{zx}^e = \frac{V^2 \{7L^2 + \nu(1-\beta)\tau[-17 + (7-10\beta)(\nu\tau/L^2)]\}}{2\nu} + \nu. \end{aligned}$$

The perturbations in (4.7) decay if the operator $\nu_{\alpha\beta} \tilde{\partial}_\alpha^2 \tilde{\partial}_\beta^2$ is negative. The condition of stability of the system is obtained by introducing the Reynolds number $Re = VL/\nu$, the Deborah number $De = V\tau/L$ and rewriting (4.7) in Fourier space:

$$\begin{aligned} (2 - Re^2 \beta^2 + 3(1-\beta) De Re + (2\beta+1)(1-\beta) De^2) s^2 + (4 + 7 Re^2 + 17(\beta-1) De Re \\ + (10\beta-7)(\beta-1) De^2) s + 2 > 0 \quad \forall s \geq 0. \end{aligned} \tag{4.8}$$

Here, $s^{1/2} = \tan \theta$, and θ is the angle between the perturbation and the basic flow, i.e. $\theta = 0$ corresponds to longitudinal perturbations, $\theta = \pi/2$ to transverse perturbations. The stability diagram in the Re – De plane is given in figure 2 (note that the topology of the phase space changes above $\beta_c \equiv 7/10$).

Two types of instabilities are predicted by our multiple-scale analysis:

(i) Hydrodynamic-like transverse instabilities take place for sufficiently large values of the Reynolds number, that is above the upper critical line in figure 2(a). In particular, we observe that the critical Reynolds number is an increasing function of the Deborah number: the elastic component tends to stabilize the flow. We can

interpret such behaviour as a prelude to the drag reduction effect observed in the fully turbulent regime (Boffetta *et al.* 2004). The lowest critical Reynolds number for such instabilities is attained for the Newtonian case ($De=0$), where we recover the well-known result that the Kolmogorov flow is linearly stable below $Re_c = \sqrt{2}$ (Meshalkin & Sinai 1961).

(ii) Purely elastic instabilities emerge for sufficiently high values of the Deborah number and small Reynolds numbers (bottom-right region of figure 2a), that is instabilities that arise for purely elastic effects. Those instabilities were discussed in Shaqfeh (1996) and Groisman & Steinberg (1996, 1997, 1998a, b, 2004) for curvilinear streamlines. The present case is, to our knowledge, the first evidence of elastic instabilities for rectilinear streamlines.

Note that in this case the direction of the most unstable mode is at a small angle with respect to the basic flow, at variance with the purely hydrodynamic transverse instabilities.

5. Generalization to finite Schmidt numbers

Adding a stress diffusion term $\kappa \partial^2 \sigma$ to the equation of motion for the conformation tensor (2.2) was suggested by Sureshkumar & Beris (1995b) to avoid Hadamard instabilities which may emerge when (2.2) and (2.4) are integrated numerically. Such instabilities are triggered when the positive definiteness of the conformation tensor is lost due to the accumulation of numerical errors. How does the artificial diffusivity alter the stability portrait? We can address this question by exploiting the multiple-scale expansion to obtain an analytical answer.

The results shown in the previous section have been obtained for an infinite Schmidt number $Sc = \nu\beta/\kappa$, where we recall that $\nu\beta$ is the solvent viscosity and κ the stress diffusivity. The latter appears on the right-hand side of (4.3) as an extra term $\kappa \partial^2 \zeta$. The analysis proceeds exactly as in the case $\kappa=0$. A source of technical difficulty is that the equations stemming from (4.3) now have a differential character, rather than algebraic as for $\kappa=0$, making the computation more cumbersome and tedious. However, the final result is still a diffusion equation like (4.7), with an eddy-viscosity tensor dependent on the Schmidt number. The resulting stability portrait for the hydrodynamic regime is shown in figure 3 for two different values of Sc . The case $Sc = \infty$ (i.e. $\kappa=0$) has been treated in the previous section, where it has been shown that the multiple-scale expansion provides reliable predictions up to Deborah numbers of order unity.

From figure 3 it is evident that the presence of the diffusivity reduces the stabilizing action of the polymers. In plain words, a non-zero stress diffusion in the equation of motion for the conformation tensor brings the system back toward the Newtonian behaviour. The physical reason is quite intuitive: the presence of a non-vanishing diffusivity tends to destroy the alignment between the stretching directions and the polymers, wiping out their capability to interact with the flow by selecting preferential orientations and making them behave, in practice, as point particles. The tendency to reach this limit for $Sc \ll 1$ has been observed in our computations and simulations (not shown).

6. Numerical analysis

For a plane parallel flow such as the basic flow of §3 it is possible to compute the exact, linear, rate of growth of a perturbation with arbitrary wavenumber, by

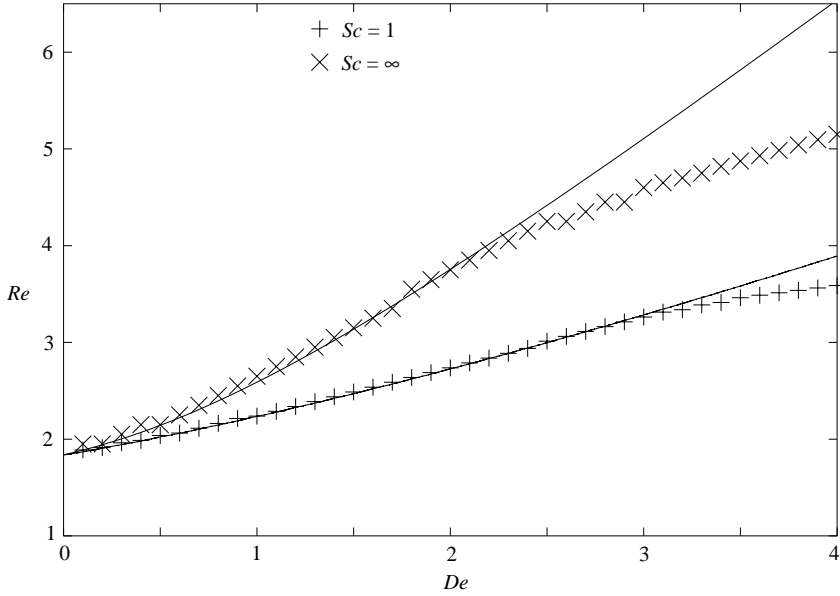


FIGURE 3. The stability portrait for finite Schmidt numbers. Symbols represent the numerical result based on the Arnoldi method, whereas solid lines are the prediction for large-scale instabilities.

means of a procedure that closely resembles the derivation of the Orr–Sommerfeld equations. Additionally, this will allow us to check if the first unstable modes are localized at the large scales and the onset of the instability of the laminar flow can be captured by the multiple-scale analysis developed in § 4.

The starting point is again the set of equations (4.1)–(4.3). Neglecting the nonlinear terms we have to deal with a set of linear partial differential equations with periodic boundary conditions. The first step is to take the Fourier transform of the perturbations \mathbf{w} and $\boldsymbol{\zeta}$ (denoted, respectively, by $\hat{\mathbf{w}}$ and $\hat{\boldsymbol{\zeta}}$), e.g.

$$w_x = \partial_z \psi \mapsto \hat{w}_x = ik_z e^{i(\mathbf{k} \cdot \mathbf{x} - ct)} \hat{\psi}(k_x, k_z), \quad (6.1)$$

$$w_z = -\partial_x \psi \mapsto \hat{w}_z = -ik_x e^{i(\mathbf{k} \cdot \mathbf{x} - ct)} \hat{\psi}(k_x, k_z), \quad (6.2)$$

$$\zeta_{ij} \mapsto e^{i(\mathbf{k} \cdot \mathbf{x} - ct)} \hat{\zeta}_{ij}(k_x, k_z). \quad (6.3)$$

Accordingly, the equation for the vorticity, $\hat{\omega} \equiv (k_x^2 + k_z^2) \hat{\psi}$, and for $\hat{\boldsymbol{\zeta}}$ are easily derived from (4.1)–(4.3). For the sake of brevity, we report here the equation for $\hat{\omega}$ only:

$$\begin{aligned} & -\frac{iV k_x}{2L^2} [L^2 k_x^2 + (L k_z - 1)^2 - 1] \hat{\psi}(k_x, k_z - 1/L) - \nu \beta (k_x^2 + k_z^2)^2 \hat{\psi}(k_x, k_z) \\ & - \frac{iV k_x}{2L^2} [L^2 k_x^2 + (L k_z + 1)^2 - 1] \hat{\psi}(k_x, k_z + 1/L) + \frac{\nu(1-\beta) k_x k_z}{\tau} \hat{\zeta}_{xx}(k_x, k_z) \\ & - \frac{\nu(1-\beta)}{\tau} ((k_x^2 - k_z^2) \hat{\zeta}_{xz}(k_x, k_z) - k_x k_z \hat{\zeta}_{zz}(k_x, k_z)) = -i c (k_x^2 + k_z^2) \hat{\psi}(k_x, k_z). \end{aligned} \quad (6.4)$$

Equations with a similar structure hold for $\hat{\boldsymbol{\zeta}}$ as well. The complete set of equations constitutes an infinite hierarchy of linear algebraic equations with non-constant coefficients, which shows a foliation in terms of k_x . Upon truncating all modes $|k_z| > k_{max}$, for each k_x , we end up with a closed linear system of $4(2k_{max} + 1)$ equations

of the form

$$\mathbf{A}\boldsymbol{\phi} = c\mathbf{B}\boldsymbol{\phi}, \quad (6.5)$$

where $\boldsymbol{\phi} = \phi_p(k_x)$ ($p \in [1, 2k_{max} + 1]$) is a vector constructed from $\hat{\psi}$ and $\hat{\xi}$ and \mathbf{A} and \mathbf{B} are two $(2k_{max} + 1) \times (2k_{max} + 1)$ matrices. A particularly convenient choice is to arrange the fields in the form

$$\phi_{4k_z+4k_{max}+1}(k_x) = \hat{\psi}(k_x, k_z), \quad (6.6)$$

$$\phi_{4k_z+4k_{max}+2}(k_x) = \hat{\xi}_{xx}(k_x, k_z), \quad (6.7)$$

$$\phi_{4k_z+4k_{max}+3}(k_x) = \hat{\xi}_{xz}(k_x, k_z), \quad (6.8)$$

$$\phi_{4k_z+4k_{max}+4}(k_x) = \hat{\xi}_{zz}(k_x, k_z), \quad (6.9)$$

for k_z integer and $k_z \in [-k_{max}, k_{max}]$. With this choice, the matrix \mathbf{B} turns out to be diagonal and \mathbf{A} is band diagonal: only $(8/L) - 1$ upper-diagonal and $(8/L) + 2$ sub-diagonal survive. Note that these numbers do not depend on k_{max} . The matrix \mathbf{B} has no null diagonal elements, and can be inverted:

$$\mathbf{B}^{-1}\mathbf{A}\boldsymbol{\phi} = c\boldsymbol{\phi}. \quad (6.10)$$

To obtain non-trivial solutions for $\boldsymbol{\phi}$, we are thus reduced to a standard eigenvalue problem, whose eigenvalues, $c(k_x)$, give the dispersion relation.

An effective solution to our eigenvalue problem is to use Krylov subspace methods for computing a subset of the eigenvalues. Here, we use the Arnoldi method, which has been successfully applied to the linear stability of Newtonian coating flows by Cristodoulou & Scriven (1988) and for viscometric viscoelastic flows by Sureshkumar & Beris (1995a). This method consists of the generation, via a Krylov sequence, of a system of reduced dimension whose eigenvectors approximate those of the whole system. The Arnoldi method is the generalization to asymmetric eigenvalue problems of the Lanczos algorithm for symmetric matrices, which is proved convergent (see e.g. Parlett 1980). This procedure yields the whole spectrum of eigenvalues $c(k_x)$ for every k_x . The stability region for a given set of parameters is defined by the condition $\max\{\text{Im}[c(k_x)]\} < 0$ for every k_x .

To obtain the results reported in figures 1 and 3 (triangles) we worked in a bi-periodic square box of side 2π with $L = 2\pi/64$ and $k_{max} = 512$. Larger values of both L^{-1} and k_{max} did not produce appreciable differences in the results.

Some remarks on figure 1 are useful. Up to $De \simeq 2.3$ (for $\beta = 0.77$), the marginal curve obtained by the multiple-scale expansion is practically indistinguishable from the one obtained by the numerical solution of the full linearized equations. For larger Deborah numbers, multiple-scale analysis fails; this is the fingerprint of the lack of scale separation between the basic Kolmogorov flow and the perturbations. For large elasticity the leading instabilities do not occur at large scales: this is the realm of elastic instabilities, the first step toward the elastic turbulence regime (Groisman & Steinberg 2000).

7. Conclusions

We have investigated the linear stability of a viscoelastic fluid flowing in a channel with periodic boundary conditions. The flow is maintained by an external source and, for the particular choice $\mathbf{f} = (F_0 \cos(z/L), 0)$, it gives rise to the well-known Kolmogorov flow. Under the hypothesis that the most unstable perturbations evolve on scales much larger than L , we exploited an asymptotic perturbative strategy (the

multiple-scale expansion) to obtain an effective equation for the temporal evolution of the large-scale perturbation. The stability problem is thus reduced to the study of the sign of the eddy viscosity appearing in the large-scale equation.

Two different kinds of instabilities are captured by the multiple-scale expansion: (i) hydrodynamic-like instabilities that, in the limit of small elasticity, give the well-known $Re_c = \sqrt{2}$ corresponding to the Newtonian limit of the theory; (ii) purely elastic instabilities occurring for large values of the elasticity. The major effect of elasticity on hydrodynamic instabilities is to increase their critical Reynolds number. In plain words, polymers stabilize the flow, a prelude to drag reduction (Govindarajan *et al.* 2001; Stone *et al.* 2002).

Our results hold for finite Schmidt numbers as well. On decreasing Sc , the effect of stabilization reduces and for $Sc \rightarrow 0$ polymers behave as a suspension of spherical particles. Finally, our perturbative predictions have been corroborated by numerical analysis carried out on the original differential equations for the perturbations, by means of the Arnoldi method. The hypothesis of scale separation is verified up to Deborah numbers of order unity. For larger De , scale separation does not hold and multiple-scale methods fail. Nonetheless, at least qualitatively, the occurrence of purely elastic instabilities is captured by the asymptotic expansions.

This work has been supported by Cofin 2003 “Sistemi Complessi e Problemi a Molti Corpi” (AM), and by the European Networks “Stirring and Mixing” HPRN-CT2002-00300 (AC) and “Non-ideal turbulence” HPRN-CT-2000-00162 (MV). Numerical simulations have been performed at CINECA (INFM parallel computing initiative).

REFERENCES

- ARNOLD, V. I. & MESHALKIN, L. 1960 A. N. Kolmogorov’s seminar on selected problems of analysis (1958–1959). *Uspekhi Mat. Nauk* **15**, 247–250.
- BENSOUSSAN, A., LIONS, J.-L. & PAPANICOLAOU, G. 1978 *Asymptotic Analysis for Periodic Structures*. North-Holland.
- BIRD, R. B., HASSAGER, O., ARMSTRONG, R. C. & CURTISS, C. F. 1987 *Dynamics of Polymeric Liquids*. Wiley-Interscience.
- BOFFETTA, G., CELANI, A. & MAZZINO, A. 2004 Drag reduction in the turbulent Kolmogorov flow. *Phys. Rev. E* (submitted).
- CRISTODOULOU, K. N. & SCRIVEN, L. E. 1988 Finding leading modes of a viscous free surface flow: an asymmetric generalized eigenproblem. *J. Sci. Comput.* **3**, 355–406.
- DRAZIN, P. G. & REID, W. D. 1981 *Hydrodynamic Stability*. Cambridge University Press.
- GOVINDARAJAN, R., L’VOV, V. S. & PROCACCIA, I. 2001 Retardation of the onset of turbulence by minor viscosity contrasts. *Phys. Rev. Lett.* **87**, 174501-1–4
- GROISMAN, A. & STEINBERG, V. 1996 Couette-Taylor flow in a dilute polymer solution. *Phys. Rev. Lett.* **77**, 1480–1483.
- GROISMAN, A. & STEINBERG, V. 1997 Solitary vortex pairs in viscoelastic Couette flow. *Phys. Rev. Lett.* **78**, 1460–1463.
- GROISMAN, A. & STEINBERG, V. 1998a Elastic vs. inertial instability in a polymer solution flow. *Europhys. Lett.* **43**, 165–170.
- GROISMAN, A. & STEINBERG, V. 1998b Mechanism of elastic instability in Couette flow of polymer solutions: experiment. *Phys. Fluids* **10**, 2451–2463.
- GROISMAN, A. & STEINBERG, V. 2000 Elastic turbulence in a polymer solution flow. *Nature* **405**, 53–55.
- GROISMAN, A. & STEINBERG, V. 2004 Elastic turbulence in curvilinear flows of polymer solutions. *New J. Phys.* **6**, 29–48.
- LARSON, R. G. 1992 Instabilities in viscoelastic flows. *Rheol. Acta* **31**, 213–263.
- LUMLEY, J. 1969 Drag reduction by additives. *Annu. Rev. Fluid Mech.* **1**, 367–384.

- MESHALKIN, L. & SINAI, YA G. 1961 Investigation of the stability of a stationary solution of a system of equations for the plane movement of an incompressible viscous fluid. *J. Appl. Math. Mech.* **25**, 1700–1705.
- NADOLINK, R. H. & HAIGH, W. W. 1995 Bibliography on skin friction reduction with polymers and other boundary-layer additives. *ASME Appl. Mech. Rev.* **48**, 351–460.
- PARLETT, B. N. 1980 *The Symmetric Eigenvalue Problem*. Prentice-Hall.
- PETRIE, C. J. S. & DENN, M. M. 1976 Instabilities in polymer processing. *AIChE J.* **22**, 209–236.
- SHAQFEH, E. S. G. 1996 Purely elastic instabilities in viscometric flows. *Annu. Rev. Fluid Mech.* **28**, 129–185.
- SQUIRE, H. B. 1933 On the stability of a three-dimensional disturbances of viscous flow between parallel walls. *Proc. R. Soc. Lond. A* **142**, 621–628.
- SREENIVASAN, K. R. & WHITE, C. M. 2000 The onset of drag reduction by dilute polymer additives, and the maximum drag reduction asymptote. *J. Fluid Mech.* **409**, 149–164.
- STONE, P. A., WALEFFE, F. & GRAHAM, M. D. 2002 Toward a structural understanding of turbulent drag reduction: nonlinear coherent states in viscoelastic shear flow. *Phys. Rev. Lett.* **89**, 208301-1–4
- SURESHKUMAR, R. & BERIS, A. N. 1995a Linear stability analysis of viscoelastic Poiseuille flow using an Arnoldi-based orthogonalization algorithm. *J. Non-Newtonian Fluid Mech.* **56**, 151–182.
- SURESHKUMAR, R. & BERIS, A. N. 1995b Effect of artificial stress diffusivity on the stability of numerical calculations and the flow dynamics of time-dependent viscoelastic flows. *J. Non-Newtonian Fluid Mech.* **60**, 53–80.
- SURESHKUMAR, R., BERIS, A. N. & HANDLER, R. A. 1997 Direct numerical simulation of polymer-induced drag reduction in turbulent channel flow. *Phys. Fluids* **9**, 743–755.
- TOMS, B. A. 1949 Observation on the flow of linear polymer solutions through straight tubes at large Reynolds numbers. *Proc. 1st International Congress on Rheology* **2**, 135–141.
- VIRK, P. S. 1975 Drag reduction fundamentals. *AIChE Journal* **21**, 625–656.